Received: 19 February 2024 | Revised: 15 June 2024 | Accepted: 6 July 2024

DOI: 10.1002/aic.18541

AIChE JOURNAL

RESEARCH ARTICLE

Separations: Materials, Devices and Processes

Carbon dioxide capture by aqueous glucosamine solutions: Pilot plant measurements and a theoretical study

Iman Hami Dindar | Nicole Lutters | Eugeny Y. Kenig

Chair of Fluid Process Engineering, Paderborn University, Paderborn, Germany

Correspondence
Eugeny Y. Kenig, Faculty of Mechanical Engineering, Chair of Fluid Process Engineering, Paderborn University, Paderborn D-33098, Germany.
Email: eugeny.kenig@upb.de

Funding information
German Research Foundation, Grant/Award Number: KE 837/38-1

Abstract

A comprehensive investigation of the potential of aqueous glucosamine solutions as an eco-friendly solvent for CO_2 capture was performed. It includes an experimental study in a pilot plant setup and a theoretical analysis with a rate-based model. The model was validated against the measured column profiles of temperature and CO_2 concentration in both liquid and gas phases. Model-based parameter sensitivity studies revealed inherent challenges for an effective absorption process. A slow reaction rate and suboptimal chemical equilibrium conditions were identified as key limitations, restricting the absorption efficiency and CO_2 loading capacity of the glucosamine solution. Furthermore, an analysis of the dissociation constant of this novel absorbent was performed and its significance with respect to the (limited) performance, capability, and efficiency evaluation was highlighted.

KEYWORDS
absorption column, acid dissociation constant, Aspen custom modeler®, CO_2 capture, glucosamine, pilot plant, rate-based model

1 | INTRODUCTION

The growing concentration of carbon dioxide in the atmosphere has become a pressing global issue, contributing significantly to climate change and other environmental problems. To counteract the adverse effects of CO_2 emissions, efficient, and sustainable CO_2 capture and storage methods are required. Among CO_2 capture technologies, absorption stands out as a promising candidate due to its superior efficiency and advanced technical development. Conventional efficient solvents used for chemical (or reactive) absorption of CO_2 are alkanolamines, for example, monoethanolamine (MEA) and methyldiethanolamine (MDEA). However, they reveal certain disadvantages, for example, substantial energy consumption for solvent regeneration, toxicity, and environmental disposal difficulties. Consequently, the quest for sustainable alternative solvents remains intensive and a broad spectrum of green solvents has been discovered.[1]

Numerous studies focused on the potential application of various natural amines as industrial solvents for application in CO_2 absorption processes. For instance, solutions of different amino acid salts, such as alanine or glycine potassium, were presented as renewable, less toxic, and biodegradable alternative absorbens.[2] Alternatively, deep eutectic solvents (DES), with their low toxicity and biodegradability, were tested for possible application in CO_2 absorption.[3] Moreover, nonamine chemicals like ionic liquids[4] and potassium carbonate[5,6] are subject of ongoing research as absorbers or additives.

In recent years, glucosamine (GlcN), a naturally occurring amino sugar, has also attracted considerable attention as a potential green

Abbreviations: ACM, aspen custom modeler; AMP, 2-amino-2-methylpropanol; ASPEN, Advanced System for Process Engineering; DES, deep eutectic solvent; EMF, electromotive force; E-NRTL, electrolyte-nonrandom two-liquid model; EST, estimated; EXP, measured; GlcN, glucosamine; MDEA, methyldiethanolamine; MEA, monoethanolamine; NMR, nuclear magnetic resonance; SIM, simulated; Vol %, volume fraction.

solvent for CO_2 capture.[7] Derived from chitin—a plentiful and renewable resource found in crustacean shells—GlcN is biodegradable, nontoxic, and noncorrosive, making it a safer choice compared to traditional solvents. GlcN reacts with CO_2 in a mechanism similar to that of tertiary alkanolamines, producing HCO_3^- and protonated GlcN ($GlcNH^+$) as reaction products.[7] The reaction rate is also close to the rate of established alkanolamines like MDEA, indicating a moderately fast reaction.[8,9] This encourages further investigations of the application of GlcN as a solvent in conventional absorption columns, both experimental and model-based. The data on material properties essential for modeling and simulation is extremely scarce. In our previous study,[10] the physical and equilibrium properties of the GlcN/CO_2 system were explored. The experimental data obtained was subsequently integrated into the Aspen Properties® databank to create a material property package. This package encompasses GlcN and $GlcNH^+$ as user-defined components, along with all necessary parameters to determine the required properties of the material system.

This work represents the first comprehensive experimental and theoretical investigation of the CO_2 absorption performance of GlcN. In the experimental part, several absorption trials were conducted in a pilot plant to evaluate the absorption efficiency and CO_2 loading of the solution under varied operational conditions. This was achieved by measuring the temperature and CO_2 concentration profiles in liquid and gas phases over the height of an absorption column filled with the structured packing Montz B1.250.

In the theoretical part, a rate-based model of the absorption column developed in our previous work for conventional solvents and implemented in Aspen Custom Modeler® was modified to fit to the new material system. The reaction parameters essential for the simulation of the absorption process were determined using the created property package in Aspen Properties®.[10] The experimentally and numerically obtained absorption efficiencies and column profiles were then compared to validate the new rate-based model.

The performed analysis provides a fundamental knowledge on GlcN potential, capabilities and limitations as a CO_2 absorbent.

2 | EXPERIMENTAL

2.1 | Materials and preparations

GlcN hydrochloride with a purity of above 98.0% was purchased from CD Bioparticles, USA. Carbon dioxide (purity above 99.7%) was supplied by Air Liquide, France. Sodium hydroxide (NaOH) with a purity of above 99.0% was purchased from Carl Roth, Germany. All chemicals were used as received without further purification.

GlcN is primarily produced and sold as a salt, most commonly hydrochloride or sulfate, to enhance its stability and solubility in water for pharmaceutical and food supplement usage. Taking into account that hydrochloride inhibits the reaction with CO_2, the purchased GlcN hydrochloride was neutralized with an equimolar amount of NaOH in all experiments. The necessary amounts of GlcN hydrochloride and sodium hydroxide powder for preparing GlcN solutions at the desired concentrations were determined using a Sartorius balance with a precision of 1 g. To prevent potential powder sedimentation within column internals, the maximum concentration of the GlcN solution was limited to 0.5 M. This precaution was due to the low solubility of GlcN in water, especially in its free hydrochloride form. GlcN hydrochloride and NaOH powder were added gradually to deionized water within a stirred tank and the solution was used for further measurements once the chemicals had dissolved completely.

2.2 | Absorption trials in the pilot plant

The performance of aqueous GlcN solution as a CO_2 absorbent was experimentally investigated in a pilot plant absorption column at Paderborn University (UPB). Detailed information on this plant and related analytical methods used for measurement of liquid-phase and gas-phase compositions is given elsewhere.[11,12] In this article, the experimental technique applied to the studied solvent is briefly presented.

Because of the degradation of GlcN at high temperatures, conventional desorption is not applicable for its regeneration after CO_2 absorption. Therefore, the solution was pumped from a reservoir container into the absorption column and returned to the same container, thus mixing the fresh solution with the loaded solution after CO_2 absorption. Figure 1 shows a simplified flow sheet of the experimental setup used for the measurements in this work. For a comprehensive overview, the specification and possible operating range of the absorption column are summarized in Table 1.

For each experiment, approximately 250 L of the fresh solution was prepared and pumped into the column at a mass flow rate of 100 kg/h. It is worth noting that in the experimental procedure used, the CO_2 loading in the solution at the column top (inlet) can change over time, which leads to some deviation from the steady state. However, the hold-up of the reservoir is significantly larger than that of the column packing section, and this ensures an almost constant composition of the solution in the reservoir during the experiments. The residence time of the solution in the reservoir is estimated to be about 2.5 h, based on its hold-up and flow rate. This is significantly longer than the residence time of the solution in the column, and therefore, the process can be considered as a quasi-steady one.

To prepare the gas phase, fresh air was initially saturated with water in a prewasher. It was then mixed with a CO_2 stream at a specific flow rate to produce the flue gas with the target CO_2 concentrations of 2 and 5 vol %. The trials were conducted using aqueous GlcN solutions with three GlcN concentrations (0.1, 0.2, 0.5 M), all but one at ambient temperature (without tempering the inlet gas and liquid streams and the column). One experiment was performed at 30°C to examine the influence of higher temperatures on the process. During the experiments, five samples of both the gas and the liquid phase were collected at different column positions, including the top and sump, to determine the concentration profiles. Besides, temperature and pressure differences were measured at different column heights. A gas chromatograph was directly integrated into the plant enabling

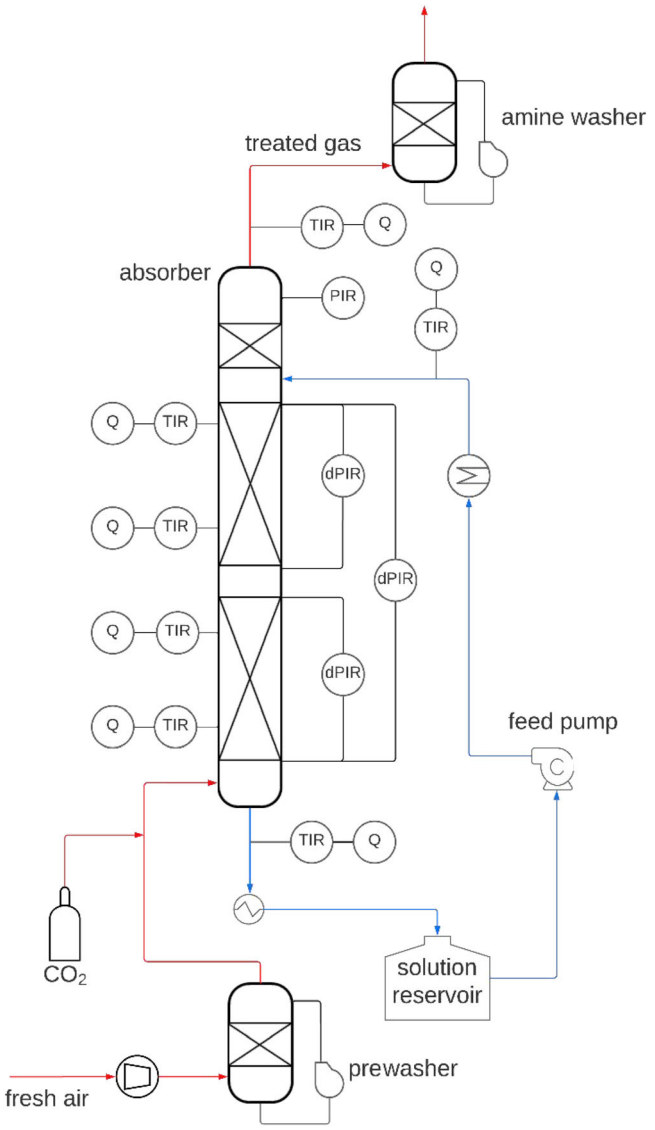

FIGURE 1 Simplified flow sheet of the absorption column at Paderborn University (UPB) used for trials with glucosamine solution as solvent. Quantities measured at the indicated locations: dPIR, differential pressure; PIR, absolute pressure; Q, gas-phase and liquid-phase CO_2 concentrations; TIR, temperature.

an online measurement of the gas-phase composition. CO_2 gas-phase mole fractions were determined using the calibration gas containing 5 vol % CO_2. This method had a relative uncertainty of 1% for the samples with CO_2 concentration close to 5 vol %, while it was doubled for the samples with concentrations close to 2 vol %. A steady state was considered as established when three consecutive measurements of the top and sump gas-phase compositions showed no deviation. Liquid samples were then collected and subsequently analyzed by titration and by the Chittick procedure[12] to determine amine and CO_2 concentrations, respectively. The relative uncertainty of the liquid CO_2 mole fractions, obtained from samples with known concentrations, was found to be 15%. This significantly higher uncertainty, compared to the results for the gas phase, is explained by the very

TABLE 1 Overview of the specification and operational conditions of the absorption column.

Parameter	Value
Column diameter	0.1 m
Packing height	2.842 m (two beds)
Type of packing	Montz B1.250, inclination angle of 45°
Gas flow rate	$30-100\ m^3/h$
Gas capacity factor	$1-3.5\ Pa^{0.5}$
CO_2 content in flue gas	1 – 15 vol%
Fluid flow rate	100 – 500 kg/h
Pressure	Atmospheric pressure
Temperature	20 – 60°C

low mole fractions, ranging from 0.0003 to 0.0015, and the lower accuracy of the measurement method used.

For all trials conducted in the pilot plant, the CO_2 absorption efficiency was determined using the following equation:

$$\psi_{abs} = \frac{y_{CO_2,in} G_{in} - y_{CO_2,out} G_{out}}{y_{CO_2,in} G_{in}}. \quad (1)$$

This quantity enables an assessment of GlcN absorption performance under different conditions. Furthermore, the total CO_2 balance within the column was analyzed to verify the acquired results. The CO_2 disbalance was calculated using Equation (2) and is presented in Table 2 along with the main process parameters and the calculated absorption efficiencies of the performed trials, labeled A–E.

$$\Delta_{CO_2} = \left| 1 - \frac{y_{CO_2,out} G_{out} + x_{CO_2,out} L_{out}}{y_{CO_2,in} G_{in} + x_{CO_2,in} L_{in}} \right| \times 100\%. \quad (2)$$

Figure 2 presents a parity plot comparing the sum of the CO_2 molar flow rates entering the absorption column with the sum of its molar flow rates leaving the column. The deviations between the inlet and outlet flow rates are below 5%, which can be regarded as satisfactory.

The calculated results presented in Table 2 reveal that the CO_2 absorption efficiency in all experiments is relatively low; this can primarily be attributed to the low GlcN concentrations in the solutions. Furthermore, no corresponding enhancement in absorption efficiency with increasing GlcN concentration was observed. Specifically, when the GlcN concentration was increased from 0.1 to 0.2 and 0.5 M while keeping all other operating conditions unchanged (experiments A, D, and E), the absorption efficiency rose only by the factors of around 1.2 and 2.1, respectively. Increasing the operational temperature to 30°C at a GlcN concentration of 0.1 M (experiments A and B) led to a decrease in absorption efficiency by a factor of 1.67. The higher temperature reduced the CO_2 loading of the solution at the outlet by a factor of 1.92, indicating lower CO_2 solubility, without any substantial improvement due to the higher reaction rate at elevated temperatures. When the CO_2 content in the flue gas was increased from 2 to 5 vol % at a

TABLE 2 Main process parameters and the calculated absorption efficiency and CO_2 disbalance for the absorption experiments with GlcN solution at pilot scale.

Experiment	A	B	C	D	E
Process parameters					
Flue gas inlet					
Volumetric flow rate [m^3/h]	35.6	36.2	38.1	37.0	38.7
Temperature [°C]	16.8	27.0	17.4	17.0	18.3
CO_2 mol fraction [–]	0.0229	0.0223	0.0529	0.0232	0.0204
Solution inlet					
Mass flow rate [kg/h]	100.03	100.01	100.00	100.01	99.98
Temperature [°C]	15.5	30.8	15.4	15.3	16.9
GlcN concentration [M]	0.1	0.1	0.2	0.2	0.5
GlcN mol fraction [–]	0.0020	0.0019	0.0030	0.0030	0.0090
CO_2 loading [mol/mol]	0.14	0.06	0.18	0.23	0.09
Outlet values					
Solution CO_2 loading [mol/mol]	0.31	0.17	0.36	0.32	0.17
Gas-phase CO_2 mol fraction [–]	0.0213	0.0211	0.0508	0.0212	0.0174
CO_2 absorption efficiency [%]	7.21	4.31	3.94	8.34	15.08
CO_2 disbalance (Equation 2) [%]	1.87	1.47	1.63	4.25	3.59

Abbreviation: GlcN, glucosamine.

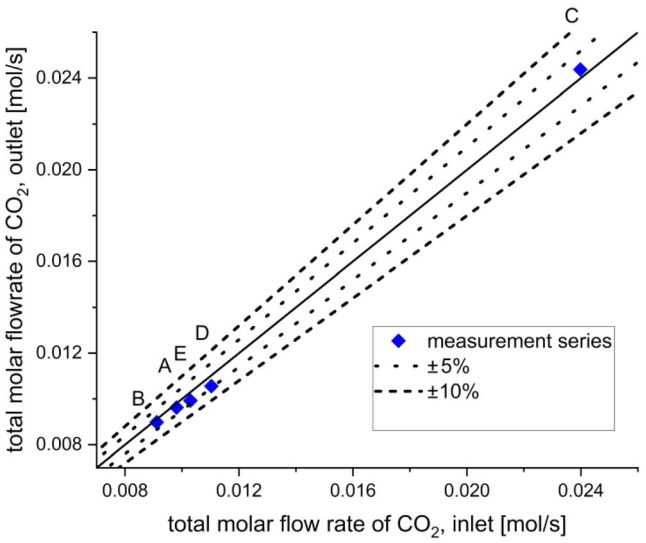

FIGURE 2 Parity plot of the total CO_2 molar flow rate entering and leaving the absorption column.

GlcN concentration of 0.2 M (experiments C and D), the absorption efficiency decreased by a factor of 2.12. This large decrease is caused by the fact that no substantial absorption enhancement could be observed for the trial with a higher inlet CO_2 concentration (experiment C) while the denominator in Equation (1) was clearly higher. This means that the excess amount of CO_2 in the gas phase could not improve the reaction performance to the expected degree.

It can be concluded that an increase in temperature adversely affects the absorption performance. Higher flue gas concentrations of CO_2 result in its higher absorbed amount; the same effect is encountered for higher inlet GlcN concentrations. Of these two effects, the second one is stronger, significantly increasing the absorption efficiency.

The experimentally obtained temperature and CO_2-concentration column profiles in both phases are presented in Section 3.2, along with the simulation results for comparison.

3 | THEORETICAL STUDIES

This section presents the theoretical investigations of the CO_2 absorption process in an aqueous GlcN solution. First, the reaction description, including rate and equilibrium constants, are determined via the estimated properties of the material system. Afterwards, a description of the development and validation of the rate-based model of the absorption column is addressed. Finally, a more detailed analysis of the underlying kinetics and equilibrium aspects is performed which explains the limited absorption performance of GlcN found both experimentally and in simulations.

3.1 | Reaction description

The reaction mechanism and description, including stoichiometry, rate and equilibrium constants, are essential for the accurate modeling and simulation of the reactive absorption process. Few studies on these issues for CO_2 absorption with GlcN solution can be found in the literature. Nuclear magnetic resonance (NMR) spectroscopy experiments by García-Abuín et al.[7] revealed a base-catalyzed reaction mechanism without carbamate formation. The reaction products are hydrogen carbonate ion (HCO_3^-) and protonated amine $GlcNH^+$. The kinetically controlled and instantaneous reactions of the CO_2–GlcN system can be summarized as follows:

$$CO_2 + GlcN + H_2O \rightarrow HCO_3^- + GlcNH^+, \quad (3)$$

$$HCO_3^- + GlcNH^+ \rightarrow CO_2 + GlcN + H_2O, \quad (4)$$

$$CO_2 + OH^- \rightarrow HCO_3^-, \quad (5)$$

$$HCO_3^- \rightarrow CO_2 + OH^-, \quad (6)$$

$$2H_2O \rightleftharpoons OH^- + H_3O^+, \quad (7)$$

$$2H_2O + CO_2 \rightleftharpoons HCO_3^- + H_3O^+, \quad (8)$$

$$HCO_3^- + H_2O \rightleftharpoons CO_3^{-2} + H_3O^+, \quad (9)$$

$$GlcNH^+ + H_2O \rightleftharpoons GlcN + H_3O^+. \quad (10)$$

In literature, two different values of the rate constant k_3 describing the forward reaction of CO_2 and GlcN (Equation 3) can be found,[8,9] yet the difference between them is small. Furthermore, for the kinetically controlled reactions described by Equations (5) and (6) and the instantaneous reactions according to Equations (7)–(9), rate and equilibrium constants are available in published data.[13,14] On the other hand, there is currently no available data on the reverse rate constant k_4 and the equilibrium constant $K_{eq,10}$ related to the protonation of GlcN in water. The reverse rate constant k_4 can be determined from the constant k_3 and the equilibrium constant of the reversible reaction $K_{eq,3-4}$:

$$K_{eq} = \frac{k_f}{k_r}, \quad (11)$$

Based on the mass action law, the equilibrium constant is directly proportional to the product of the activities of the reactants and products, each raised to the power of their stoichiometric coefficients in the reaction. Hence, the expressions for the calculation of $K_{eq,3-4}$ and $K_{eq,10}$ can be formulated as follows:

$$K_{eq,3-4} = \frac{x_{HCO_3^-}\, x_{GlcNH^+}}{x_{CO_2} x_{GlcN}\, x_{H_2O}} \times \frac{\gamma_{HCO_3^-}\, \gamma_{GlcNH^+}}{\gamma_{CO_2}\, \gamma_{GlcN}\, \gamma_{H_2O}}, \quad (12)$$

$$K_{eq,10} = \frac{x_{GlcN}\, x_{H_3O^+}}{x_{GlcNH^+} x_{H_2O}} \times \frac{\gamma_{GlcN}\, \gamma_{H_3O^+}}{\gamma_{GlcNH^+} \gamma_{H_2O}}. \quad (13)$$

The equilibrium constants can be experimentally determined at different temperatures and amine concentrations (ionic strengths), for example, via spectroscopy or electromotive force (EMF) measurements.[15,16] The values of the equilibrium constants can then be estimated from a linear extrapolation to the infinite dilution state, at which the equilibrium constant is independent of ionic strength. Alternatively, the equilibrium constant at infinite dilution can be calculated from the reference state Gibbs energies of the reactants and products, as given by Equation (14).

$$-RT \ln K_{eq}(T) = \Delta G^0_{reaction}(T) = \sum_{products} G_i^0(T) - \sum_{reactants} G_j^0(T). \quad (14)$$

The reference states are pure liquid for the solvents (water and amines) and aqueous phase at infinite dilution and 298.15 K for the solutes (ionic and molecular). The required reference state Gibbs energy of the reaction components $G_{i,j}^0(T)$ can be calculated with available equations in Aspen Properties® for all molecular and ionic species. However, this calculation requires reliable material property parameters in the software databank, specifically Gibbs energy and enthalpy of formation, as well as specific heat capacity. It is worth noting that the presence of equimolar amounts of sodium and chloride ions in the solution, resulting from the neutralization of GlcN hydrochloride, significantly increases the ionic strength of the GlcN solution. Consequently, determination of the equilibrium constant from the Gibbs energy of the components may be more accurate than a linear extrapolation from the measured constants at high ionic strengths.

In our previous work,[10] GlcN and its protonated cation was implemented into the Aspen Properties® databank and a material property package specific to the CO_2/GlcN system was developed. This package can predict the phase and chemical equilibrium of the material system via activity coefficients obtained with the Electrolyte-nonrandom two-liquid model (NRTL). Furthermore, the equilibrium constants for the implemented instantaneous reactions (Equations (7)–(10)) are determined from the reference state Gibbs free energy change, as described by Equation (14). By a regression analysis, all necessary model parameters were adjusted to the experimental data, including CO_2 solubility, heat of absorption, heat capacity, and pH values. A comprehensive overview on the developed property package and its properties can be found in the above mentioned work.[10]

In this work, we utilized the property analysis tool (property estimation for mixtures of defined composition) available in Aspen Properties® to calculate the standard state Gibbs energy, mole fraction, and activity coefficients of the components in the binary and ternary mixtures of 0.1 M aqueous GlcN solution, with and without an equimolar amount of dissolved CO_2. The calculations were conducted for the thermodynamic state of saturated liquid within a temperature range of 5 to 45°C. The equilibrium constants at each temperature, $K_{eq}(T)$, were then determined by Equation (14) and, alternatively, from the estimated composition of the GlcN–H_2O and CO_2–GlcN–H_2O mixtures using Equations (12) and (13). Both sets of results demonstrated a very close agreement, thereby confirming the consistency of the property parameters used for the calculation of the Gibbs energies and activity coefficients. Temperature-dependent formulas for the equilibrium constants were derived from the individual values by linear regression with the least squares method. Table 3 summarizes the coefficients of the equilibrium constants determined in this work for reactions involving GlcN, along with the published coefficients for other instantaneous reactions.

The reverse rate constant as function of temperature, $k_4(T)$, was calculated using Equation (11). The equilibrium constant values were obtained as described above, while the forward rate constants were determined using the published equations (cf. Table 4).

TABLE 3 Equilibrium constants of the instantaneous reactions in the CO_2 absorption in aqueous glucosamine solution, given by Equations (3), (4), (7)–(10).

$K_{eq} = A + \frac{B}{T} + C \ln T$

No.	Equilibrium constant [−]	A	B	C	Reference
1	$K_{eq,3-4}$	616.97	−20720.18	−94.88	This work
2	$K_{eq,7}$	132.90	−13445.90	−22.48	Aspen Inc.[14]
3	$K_{eq,8}$	231.47	−12092.10	−36.78	Aspen Inc.[14]
4	$K_{eq,9}$	216.05	−12431.70	−35.48	Aspen Inc.[14]
5	$K_{eq,10}$	−383.88	8542.35	57.86	This work

TABLE 4 Rate constants of the kinetically controlled reactions in the CO_2 absorption in aqueous glucosamine solution, given by Equations (3)–(6).

Arrhenius equation: $k = k_0 \exp\left(-\frac{E}{RT}\right)$

No.	Rate constant $[M^{-1}s^{-1}]$	k_o	E[cal/mol]	Reference
1	k_3	5.38×10^7	9373.4438	Gómez-Díaz et al.[8]
2	k_3	1.21×10^7	8034.6643	Sarode et al.[9]
3	k_4	2.04×10^{14}	22454.3338	From No. 1 and Equation (11)
4	k_4	4.62×10^{13}	21117.7814	From No. 2 and Equation (11)
5	k_5	4.32×10^{13}	13,249	Pinsent et al.[13]
6	k_6	2.38×10^{17}	29,451	Aspen Inc.[14]

Subsequently, the two generated data sets were employed to adjust the coefficients of the Arrhenius equation given in Table 4, specifically, the pre-exponential factor and the activation energy, through linear regression analysis. Table 4 collects all parameter values necessary for the calculation of the rate constants for the GlcN-CO_2 system, which were either determined in this study or obtained from existing literature sources.

3.2 | Rate-based model of absorption column

A rate-based model of the absorption column in Aspen Custom Modeler® (ACM), developed in our previous research for the conventional solvents, was adapted in this study to accommodate GlcN as the CO_2 absorbent. Theoretical principles and a detailed model description were outlined elsewhere (see, e.g., references[17,18]). This section provides a concise overview of the procedure for applying the model to the new material system.

In contrast to the equilibrium model, the rate-based approach involves separate balancing of the gas and liquid phases. In this approach, mass and heat transport resistances are taken into account, employing the film theory. Given the nonvolatile nature of GlcN, its reaction with CO_2 exclusively occurs in the liquid phase. This reaction was reported in the literature as moderately fast, characterized by $0.3 < Ha < 3$.[8,9] Consequently, along with the mass transfer resistance, the effect of chemical reaction should also be taken into account in the liquid film. This results in a differential component balance and a nonlinear concentration profile within the film. The differential equation describing such a profile is solved numerically, by discretization along the film width. The column is also discretized in the axial direction, while the number of required discrete elements in both axial and radial directions is evaluated in a grid independence study.

For the calculation of the physical properties and the phase equilibrium of the CO_2/aqueous GlcN system, ACM was directly linked to the property package created in the software Aspen Properties®. Specifically, the necessary physical properties for the simulations including density, viscosity, surface tension, thermal conductivity, heat capacity, molar enthalpy, and diffusion coefficient as well as the vapor–liquid equilibrium parameters activity-based K-value, activity coefficient, and Henry's constant are calculated by material property package at each temperature, pressure, and concentrations of solvent (GlcN + NaCl) and CO_2. As mentioned above, this property package is comprehensively described in our previous publication.[10]

The chemical reactions encountered in the absorption process under investigation are described by the reaction rate and equilibrium constants. The reaction parameters discussed in Section 3.1 were implemented in the model in the following way. The rate constant for the forward reaction of CO_2 with GlcN was taken from Sarode et al. (No. 2 in Table 4), resulting in a slightly higher reaction rate compared with another available approach (No. 1 in Table 4).

Equation (11) became a part of the model to determine, at each temperature, the rate constant of the reverse reaction from the forward rate constant and the equilibrium constant of the reversible reaction (No. 1 in Table 3). Furthermore, the forward and reverse rate constants of the reaction of CO_2 with OH^- ion, as given in Table 4 (No. 5 and 6), and the equilibrium constants of the dissociation reactions, as given in Table 3 (No. 2–5), were incorporated into the rate-based model.

Model parameters to describe the influence of column internals and hydraulics were determined using empirical correlations. For the Montz packing B1-250 with corrugation angle of 45°, which was also used in the experimental investigations, the following correlations were implemented in ACM. Effective mass transfer area was evaluated according to Tsai et al.[19] Mass transfer coefficients, volumetric hold-up, and pressure drop were estimated by correlations taken from Rocha et al.[20,21] Furthermore, correlations from Olujic et al.[22] for these parameters were applied and the results were compared. Due to the very low concentrations of the solvent and CO_2 investigated, the choice of the correlations has just an insignificant impact on the simulation results. Geometry parameters of the packing were determined through self-measurements, resulting in a crimp height (h) of 0.0125 m and a channel base (b) of 0.035 m. A simple relationship was implemented in the model to calculate the channel side (*s*) as the

length of the hypotenuse of a right-angled triangle; for the packing used, this value is equal to 0.0215 m. For a better overview, the parameters of the structured packing used in the rate-based model are summarized in Table 5.

For the simulation of the absorption process, the specifications of the column and its operating conditions were adopted from the pilot plant experiments (cf. Section 2.2). This enables a direct comparison between the simulation and measurement results. Figure 3 demonstrates the simulated and experimentally obtained column profiles for temperature and CO_2 concentrations in the liquid and gas phases, for 0.1 M (Figure 4A) and 0.2 M (Figure 4B) GlcN solutions. The results are shown for experiments A and B (0.1 M solution at two operating temperatures), as well as for experiments C and D (0.2 M GlcN solution and two CO_2 concentrations of 2 and 5 vol % in the flue gas) according to Table 2.

The measured values, especially the CO_2 concentrations in the liquid phase, show some scattering. It can be attributed to the limited accuracy of the measurements within the investigated narrow concentration range. Nevertheless, a good qualitative agreement between the simulated and experimental data is obvious. As can be seen in both the simulation and experimental results of Figure 3A, an increase in temperature results in reduced CO_2 mole fractions in the solution, while the concentration profiles of the gas phase demonstrate no substantial differences. Figure 3B shows that a higher CO_2 concentration in the flue gas results in an increased dissolved CO_2 amount in the solution. However, both experimental and simulated liquid CO_2 mole fractions for experiment C clearly show solution saturation in the bottom part of the column (nearly vertical curves).

Figure 4 illustrates the effects of GlcN concentration on the column profiles for both the simulated and experimental data. The measured results are obtained from the pilot plant trials A, D, and E (Table 2), with three different GlcN concentrations (0.1, 0.2, and 0.5 M) and otherwise identical operational conditions: ambient temperature and a CO_2 concentration of 2 vol % in the flue gas.

Despite the fluctuations in the experimental data, a good agreement between the simulated and experimental curves is visible. When the solvent concentration is doubled from 0.1 to 0.2 M, a subtle shift in the simulated column profiles for temperature and CO_2 mole fraction in the gas phase is encountered. However, due to the limited measurement accuracy, this shift could not be detected experimentally. On the other hand, simulated CO_2 liquid mole fractions in the 0.1 and 0.2 M solutions show an almost identical increase. As the solvent concentration grows to 0.5 M, there is a more pronounced reduction in the CO_2 content in the flue gas than for lower solvent concentrations. This leads to a more significant rise of the CO_2 concentration in the liquid phase (Figure 4B).

In general, the simulated and measured CO_2 concentrations of the liquid phase show larger deviations than those of the gas phase. One reason for this fact could be the lower measurement accuracy of the Chittick method used for the liquid samples compared to the gas chromatography for the gas phase. Moreover, the posttreatment of the liquid samples may also have some influence on the results. The liquid samples were analyzed after the absorption trials, which can alter the CO_2 concentration due to the temporal degradation of GlcN. This effect can be more pronounced at higher GlcN concentrations, as an accelerated degradation rate of the solution comes into play.

Figure 5 presents the parity plot of the absorption efficiencies determined from simulated and experimental data. In trials B and C, the deviation between the experimental and simulated absorption efficiencies is around 30%. For the remaining experiments, this deviation is below 20%, reaching its lowest value at 3.78% in trial E, which is conducted with the highest concentration of GlcN. The relatively large discrepancies between the simulated and experimental results can be attributed to the inherent complexity of measurements and model-based predictions in a dilute state. In diluted mixtures, the uncertainty factors, including analytical and measurement errors, uncertain methodologies and parameters, collectively exert a more pronounced influence on the accuracy, both in experiment and in simulation. Nevertheless, the model reveals a reasonable agreement with the experimental data so that the special characteristics of the process with GlcN can be adequately mapped by the simulation. Therefore, the developed rate-based model can be used for further simulation-based studies.

TABLE 5 Parameters of the Montz structured packing B1-250 used in the rate-based model of the absorption column.

Parameter	Value
Specific surface area of packing, m^2/m^3	250
Void fraction, –	0.97
Inclination angle, °	45
Crimp height, m	0.0125
Channel base, m	0.035
Channel side, m	0.0215

3.3 | Evaluating GlcN as a potential CO_2 absorbent

In this section, a detailed evaluation of GlcN as a potential CO_2 absorbent is given, based on both developed simulation tools—the property package and the rate-based model. As a first step, a parametric study with the validated rate-based model was carried out to consider the effect of solvent and CO_2 concentrations on the process. This analysis was also aimed to explore the influence of the low reaction rate on the overall process performance. Several simulations of CO_2 absorption were performed with 0.1, 0.2, and 0.5 M GlcN solutions, with the CO_2 concentrations of the flue gas set at 2 and 5 vol %. To ensure a straightforward comparison, other operational parameters were kept constant at the following values: a temperature of 15°C, flow rates of the flue gas, and the solvent of 38.7 m^3/h (gas load factor of 1) and 100 kg/m^3, respectively, with a zero CO_2 loading of the inlet solutions. Furthermore, the effect of residence time on the absorption performance was examined to determine the maximum attainable absorption capacity of GlcN. This was achieved by varying the column height for each set of conditions. The residence time was calculated

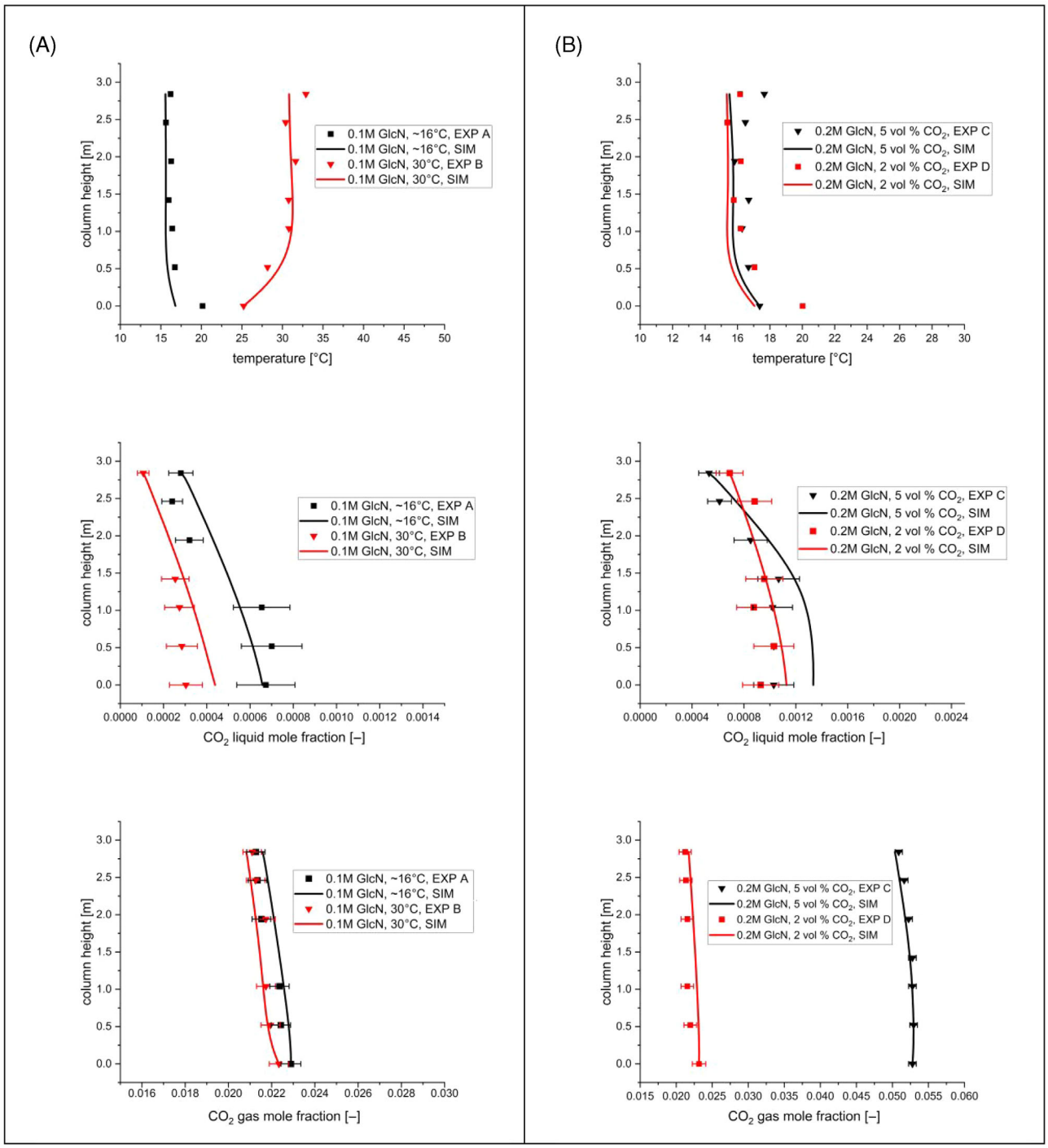

FIGURE 3 Experimental (EXP) and simulated (SIM) column profiles for temperature and CO_2 concentration in liquid and gas phases, for 0.1 M glucosamine (GlcN) solution corresponding to trials A and B in pilot plant (A) and for 0.2 M GlcN solution corresponding to trials C and D in pilot plant (B).

based on the volumetric hold-up of the column, estimated using correlations from Rocha et al.[20] for Montz packing B1.250, and considering the volumetric flow rate of the solution at the column outlet. The simulated absorption efficiency and CO_2 loading of the solution are shown in Figure 6.

The presented results for 2 vol % CO_2 concentration of the flue gas (dashed lines in Figure 6) demonstrate a significant increase of the absorption efficiency and CO_2 loading of the solvent with longer residence time. This enhancement is directly related to the low reaction rate of the system, yet it is limited by the equilibrium composition. Notably, the maximum CO_2 loading of the solutions does not exceed the value of 0.5, which shows that even at an equilibrium state, more than half of the GlcN molecules do not participate in the reaction. Increasing the CO_2 concentration of the flue gas to 5 vol % (solid lines

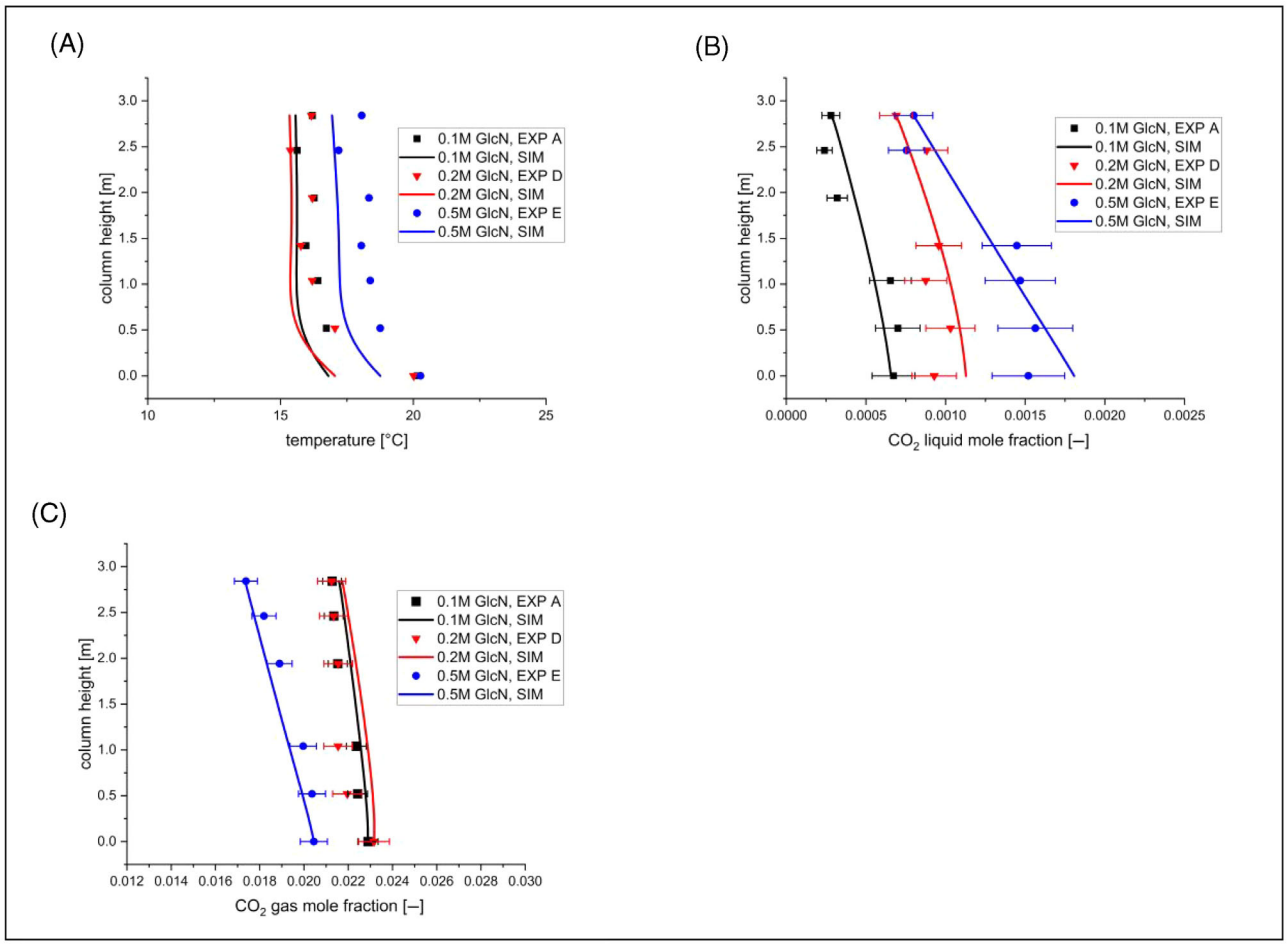

FIGURE 4 Experimental (EXP) and simulated (SIM) column profiles for temperature (A), CO_2 concentration in liquid (B) and gas (C) phase for 0.1, 0.2 and 0.5 M glucosamine (GlcN) solutions corresponding to trials A, D, and E in pilot plant.

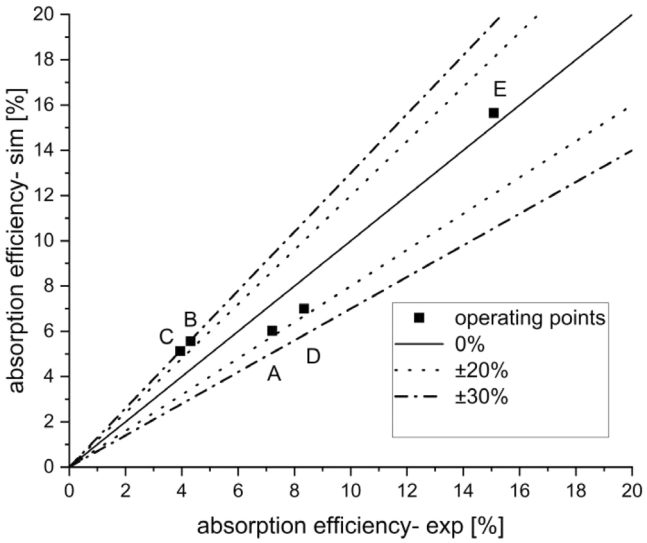

FIGURE 5 Parity plot for the calculated absorption efficiencies: Simulated (sim) against experimental (exp) values.

in Figure 6) reduces the residence time required for saturation of the solution and also slightly increases its maximum CO_2 loading. Nonetheless, the absorption efficiencies decrease because the solution cannot capture the increased amount of CO_2 properly. This suggests that the chemical equilibrium substantially limits the extent of the reaction between GlcN and CO_2, while it can be shifted toward products by increasing the concentration of reactants, namely both the solvent and the CO_2. Given that GlcN does not directly react with CO_2, this limitation likely stems from its degree of protonation in water, forming ion OH^- to bound sour gases. Commonly used tertiary and sterically hindered alkanolamines, such as MDEA and aminomethyl propanol (AMP), follow the same indirect reaction mechanism as GlcN. However, they do not exhibit such a limited absorption capacity caused by a suboptimal chemical equilibrium. This particular equilibrium characteristic of GlcN can be compared to that of conventional solvents using the acid dissociation constant (pK_a), which is determined by the following equation:

$$pK_a = -\log_{10}\frac{[R-NH_n][H_3O^+]}{[R-NH_{n+1}^+]}. \quad (15)$$

The square bracket represents the true molar concentration of components after dissociation reaction. The degree of protonation of amines in the aqueous phase can be expressed in terms of the acid dissociation constants of their protonated cations (conjugated acids).

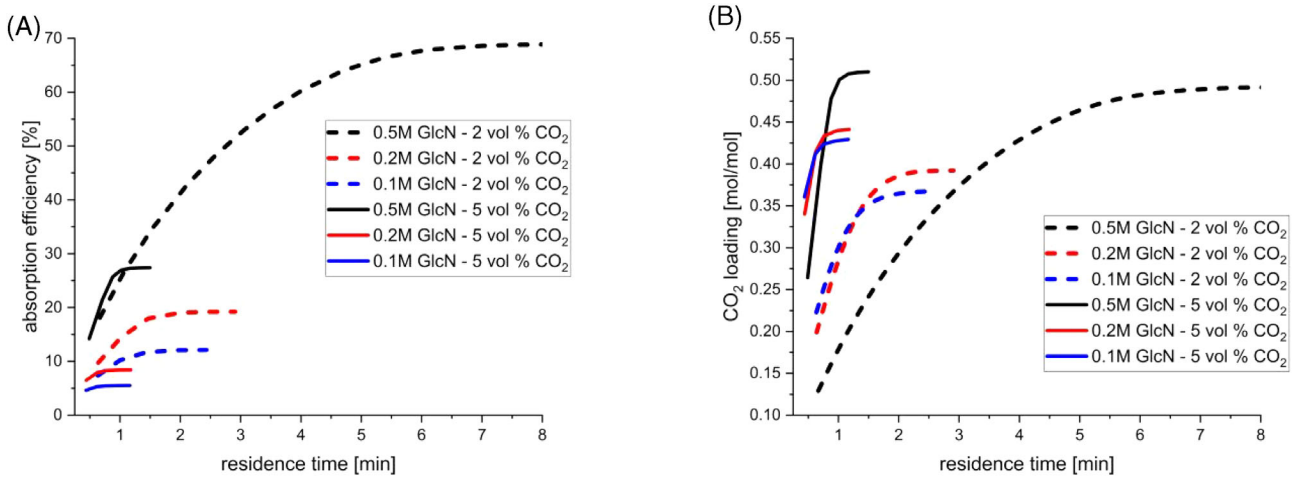

FIGURE 6 Absorption efficiency (A) and CO_2 loading of the solution (B) obtained from the parametric study using the rate-based model of the absorption column for simulations under various glucosamine (GlcN) and CO_2 concentrations and different residence times.

As can be deduced from Equation (15), a higher degree of protonation correlates with a higher pK_a value of the amine.

According to the literature,[15,23] most amines used for CO_2 capture have pK_a values in the range of 8.5–11 at 25°C, characterizing them as moderately strong bases. Strong bases like sodium hydroxide dissociate completely in an aqueous solution. On the other hand, moderately strong and weak bases dissociate only partially in pure water, depending on their pK_a values. The presence of an acidic component in the solution, such as carbonic acid (from the solvation of CO_2), promotes the amine protonation by providing more H_3O^+ protons. For instance, MDEA, a moderately strong base ($pK_a = 8.5$[23]), can be completely protonated by reaction with weak carbonic acid ($pK_{a,1} = 6.35$ to form bicarbonate ion[24]) and, therefore, can absorb CO_2 gas up to a loading of 1 mol/mol. In contrast, in a weak acid–weak base reaction, both components dissociate only partially in the solution, reaching an equilibrium point between the reactants and products. This behavior is similar to the observed limited CO_2 absorption in GlcN solutions. Along these lines, an analysis of the dissociation constant of novel absorbents can be instrumental in evaluating their capacity and efficiency in CO_2 capture.

As no experimental data on the acid dissociation constant of GlcN is available in the literature, we estimated it in this work at 25°C using Aspen Properties®. The pK_a values were calculated using Equation (15), based on the estimated composition of the aqueous GlcN solution at various apparent amino sugar concentrations. This analysis followed the same procedure as that used to determine the equilibrium constant of the protonation reaction, as described in Section 3.1. Since the GlcN solution contains equimolar sodium and chloride ions from the neutralization of GlcN hydrochloride salt, its ionic strength is relatively high compared with conventional amine-based solvents with the same concentration. The ionic strength depends on the molar concentration c and the charge number Z of all ionic species dissolved in the solution, as expressed by Equation (16):

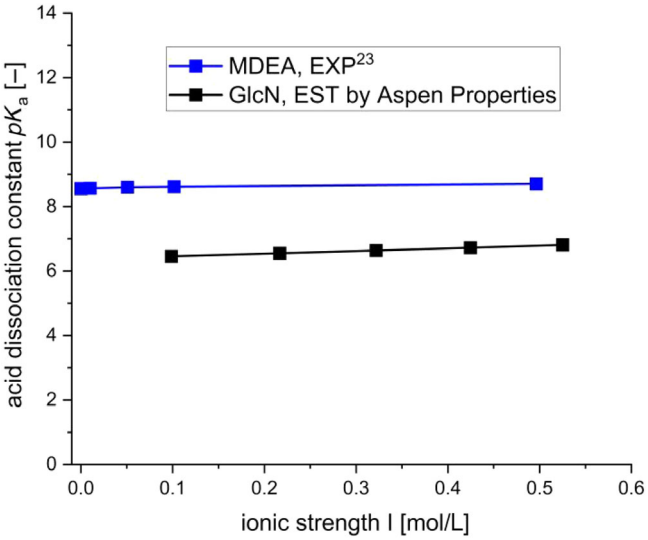

FIGURE 7 Acid dissociation constant (pK_a) of glucosamine estimated by Aspen properties® (EST), together with published values (EXP) of methyldiethanolamine (MDEA) at different ionic strength of the solution.

$$I = \frac{1}{2}\sum_{i=1}^{n} c_i Z_i^2. \quad (16)$$

This ionic strength, which increases with raising GlcN concentration and accordingly higher amount of Na^+ and Cl^-, influences the dissociation constant of amine by altering the activity coefficients of the components. Therefore, for a reasonable comparison of GlcN with other basic solvents, the pK_a values should be plotted against the ionic strength of the solution. The obtained dissociation constants of GlcN are presented in Figure 7, which also includes published data for the conventional solvent MDEA. The literature data were obtained by Kim et al.[23] at an MDEA concentration of 0.01 mol/kg-water, with

various amounts of NaCl as a background salt to investigate the effect of ionic strength on the dissociation constant.

The comparison of the curves in Figure 7 reveals that GlcN, with a mean pK_a value of about 6.5, has a significantly weaker basic strength than the common CO_2 absorbents. As mentioned earlier, this characteristic results in only partial protonation of the amino group during its reaction with CO_2. It is noteworthy that GlcN is entirely protonated in its primary hydrochloride salt form, due to the reaction with a strong acid. This fact confirms that its limited CO_2 absorption performance is solely due to the weak acid–weak base nature of the reaction with carbonic acid, hence, other potential factors like a steric hindrance or high mass transfer resistance can be ruled out. The partial dissociation of both a weak acid and a weak base as reactants leads to their relatively high concentration at the chemical equilibrium compared to the concentration of the ionic products. Increasing the concentration of the reactants shifts the equilibrium toward reaction products according to Le Chatelier's principle. Given that GlcN exhibits weaker basic strength (its tendency to accept protons) compared with the acidic strength of carbonic acid (its tendency to release protons), it can be considered to be the limiting component in this reaction. This assumption is supported by both measurements and simulations of the absorption process, while an increase in GlcN concentration resulted in a more pronounced enhancement of absorption efficiency and CO_2 loading in the solution.

Finally, it appears reasonable to compare the absorption performance of low-concentration GlcN with that of conventional solvents. Since there are no published experimental data for other amines at low solution concentrations, a simulative analysis was conducted for 0.5 M MDEA solution and flue gas of 2 vol % with the rate-based model available within the Aspen Plus® package.[14] The column specifications and operating conditions were identical to those assumed for GlcN and introduced in the beginning of this section. The performance of GlcN and MDEA is illustrated in Figure 8 which shows the dependence of absorption efficiency and CO_2 loadings on the residence time. Here, the influence of reaction kinetics and equilibrium can be recognized. A higher reaction rate of GlcN is advantageous for the residence times of up to 10 min resulting in a superior absorption efficiency and a higher loading. At higher residence times (over 18 min), MDEA becomes preferrable. Note that relatively short residence times—ranging from few seconds to few minutes—are typical for industrial absorption columns. Considering that absorption capacity of commonly used primary amines like MEA are limited similarly to GlcN, the latter can be judged as a candidate solvent with a reasonable potential for the CO_2 absorption.

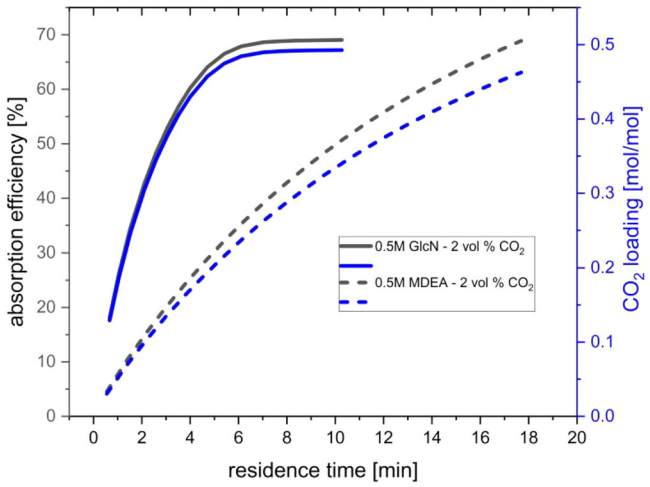

FIGURE 8 Absorption efficiency and CO_2 loading of the 0.5 M glucosamine (GlcN) and methyldiethanolamine (MDEA) solutions with entering flue gas of 2 vol % CO_2 for different residence times. Solid lines: glucosamine, dash lines: MDEA; black lines: absorption efficiency, blue lines: CO_2 loading.

Beyond the theoretical analysis presented in this section, additional experimental studies on the dissociation constant and the CO_2 solubility at elevated GlcN concentrations are essential. These investigations are critical to evaluate GlcN suitability comprehensively for industrial-scale CO_2 capture applications. Besides, absorption of sour gases with higher acidity in the aqueous phase, such as sulfur dioxide ($pK_a = 1.85$[24]), presents a promising field of application for GlcN. The reaction with stronger acids enables a complete protonation of GlcN, potentially leading to a higher absorption efficiency and a gas loading capacity of up to 1 mol/mol.

4 | CONCLUSIONS

A detailed investigation of the potential of aqueous GlcN solution to serve as an industrial-scale CO_2 capture solvent was carried out. Pilot plant experiments were complemented by rate-based column modeling and simulations. The experimental and simulation results provided substantial insights and illuminated both the potential and limitations of GlcN as a CO_2 absorbent. Despite the environmental advantages of GlcN over conventional solvents, the identified key limitations, above all its slow reaction rate and sub-optimal chemical equilibrium characteristics, reduce the maximum CO_2 loading achievable in the solution.

The importance of the dissociation constant (pK_a) of GlcN, a crucial parameter in assessing the suitability of a novel CO_2 absorbent, was highlighted. The weak base nature of GlcN, reflected in its pK_a value, implies a partial protonation in reaction with carbonic acid, thus limiting its CO_2 absorption capacity. Increasing the solvent concentration can shift the reaction equilibrium, thereby enhancing the efficiency of CO_2 capture. Furthermore, a simulative comparison of the absorption efficiency and loading capacity performed for low-solvent GlcN and MDEA solutions showed superior GlcN performance for short residence times.

This study paves the way for future research toward overcoming the limitations of GlcN as a CO_2 absorbent to exploit its eco-friendly attributes. To improve its CO_2 absorption performance, further investigations on potential process modifications, such as optimizing the

GlcN concentration or exploring synergistic blends, are recommended. The application of GlcN for the purification of flue and process gases with higher acidity can also be considered.

NOMENCLATURE

Parameters and symbols

b	channel base of structured packing, m
c	apparent (prereaction) concentration, M
E	activation energy of the Arrhenius equation, cal/mol
G	Gibbs energy, cal/mol
G	total molar flow of the gas phase, mol/s
h	crimp height of structured packing, m
Ha	Hatta number, –
I	ionic strength, M
k	reaction rate constant, $1/(\mathrm{M\,s})$
k_0	pre-exponential factor of the Arrhenius equation, –
K_{eq}	reaction equilibrium constant, –
L	total molar flow of the gas phase, mol/s
pK_a	acid dissociation constant of conjugate amine, –
R	gas constant, 1.9872, $\mathrm{cal/(mol\,K)}$
s	channel side of structured packing, m
T	temperature, K
x	mol fraction in liquid phase, –
y	mol fraction in gas phase, –
Z	charge number of ionic species, –

Greek letters

γ	activity coefficient, –
ψ	absorption efficiency, –

Subscripts

abs	absorption
c	critical point
f	forward reaction
g	gas
i,j	products and reactants of the chemical reaction
in	inlet
out	outlet
r	reverse (backward) reaction

Superscripts

0	reference state

AUTHOR CONTRIBUTIONS

Eugeny Y. Kenig: Writing – review and editing; conceptualization; supervision. **Iman Hami Dindar:** Conceptualization; investigation; writing – original draft; methodology; validation; software. **Nicole Lutters:** Conceptualization; writing – review and editing.

ACKNOWLEDGMENTS

The financial support provided by the German Research Foundation (DFG, KE 837/38-1) is gratefully acknowledged. Open Access funding enabled and organized by Projekt DEAL.

DATA AVAILABILITY STATEMENT

The numerical data used for Figures 2–8 are tabulated in the Supporting Information. The code for the rate-based model used in this work was developed in collaboration with industrial partners and hence cannot be shared because of confidentiality reason. The reliability and reproducibility of the reported pilot plant data have been ensured in our recent experimental works[11,12]; for the simulated data, this has been done in the recent numerical studies.[17,18]

ORCID

Iman Hami Dindar https://orcid.org/0009-0005-2276-468X
Nicole Lutters https://orcid.org/0009-0006-7828-8448
Eugeny Y. Kenig https://orcid.org/0000-0002-7521-9408

REFERENCES

1. Nematollahi MH, Carvalho PJ. Green solvents for CO_2 capture. *Curr Opin Green Sustain Chem*. 2019;18:25-30.
2. Sang Sefidi V, Luis P. Advanced amino acid-based technologies for CO_2 capture: a review. *Ind Eng Chem Res*. 2019;58(44):20181-20194.
3. Gu Y, Hou Y, Ren S, Sun Y, Wu W. Hydrophobic functional deep eutectic solvents used for efficient and reversible capture of CO_2. *ACS Omega*. 2020;5(12):6809-6816.
4. Wappel D, Gronald G, Kalb R, Draxler J. Ionic liquids for post-combustion CO_2 absorption. *Int J Greenhouse Gas Control*. 2010;4(3):486-494.
5. Thiele R, Faber R, Repke J-U, Thielert H, Wozny G. Design of industrial reactive absorption processes in sour gas treatment using rigorous modelling and accurate experimentation. *Chem Eng Res Des*. 2007;85(1):74-87.
6. Isa F, Zabiri H, Harun N, Shariff AM. CO_2 removal via an environmental green solvent, K_2CO_3-glycine (PCGLY): investigative analysis of a dynamic and control study. *ACS Omega*. 2022;7(22):18213-18228.
7. García-Abuín A, Gómez-Díaz D, Navaza JM. Characterization of carbon dioxide capture by glucosamine: liquid phase speciation and degradation. *J Ind Eng Chem*. 2014;20(4):2272-2277.
8. Gómez-Díaz D, Navaza JM. Kinetics of carbon dioxide absorption into aqueous glucosamine solutions. *AIChE J*. 2008;54(1):321-326.
9. Sarode UK, Vaidya PD, Kenig EY. Glucosamine for CO_2 capture: absorption kinetics, promoted absorption rate, and comparison with other amino sugars. *Ind Eng Chem Res*. 2023;62(3):1492-1498.
10. Hami Dindar I, Mirzaei M, Baumhögger E, Lutters N, Kenig EY. Experimental and theoretical investigation of CO_2 absorption in aqueous solution of glucosamine: material property and equilibrium data. *J Chem Eng Data*. 2024;69(3):824-841.
11. Hüser N, Yazgi M, Hugen T, Rietfort T, Kenig EY. Experimental and numerical characterization of a new structured packing for CO_2 capture. *AIChE J*. 2018;64(11):4053-4065.
12. Hüser N. *Untersuchung der Abscheidung von Kohlenstoffdioxid mit Alkanolaminen. Verfahrenstechnik*. Dr. Hut; 2017.
13. Pinsent BRW, Pearson L, Roughton FJW. The kinetics of combination of carbon dioxide with hydroxide ions. *Trans Faraday Soc*. 1956;52:1512-1520.
14. Aspen Technology Inc. Rate-based model of the CO_2 capture process by MDEA using Aspen plus. 2020.

15. Hamborg ES, Versteeg GF. Dissociation constants and thermodynamic properties of amines and alkanolamines from (293 to 353) K. *J Chem Eng Data*. 2009;54(4):1318-1328.
16. Ermatchkov V, Pérez-Salado Kamps Á, Maurer G. Chemical equilibrium constants for the formation of carbamates in (carbon dioxide +piperazine+water) from -NMR-spectroscopy. *J Chem Thermodyn*. 2003;35(8):1277-1289.
17. Hüser N, Schmitz O, Kenig EY. A comparative study of different amine-based solvents for CO_2-capture using the rate-based approach. *Chem Eng Sci*. 2017;157(8):221-231.
18. Huepen B, Kenig EY. Rigorous modeling and simulation of an absorption−stripping loop for the removal of acid gases. *Ind Eng Chem Res*. 2010;49(2):772-779.
19. Tsai RE, Seibert AF, Eldridge RB, Rochelle GT. A dimensionless model for predicting the mass-transfer area of structured packing. *AIChE J*. 2011;57(5):1173-1184.
20. Rocha JA, Bravo JL, Fair JR. Distillation columns containing structured packings: a comprehensive model for their performance. 1. Hydraulic models. *Ind Eng Chem Res*. 1993;32(4):641-651.
21. Rocha JA, Bravo JL, Fair JR. Distillation columns containing structured packings: a comprehensive model for their performance. 2. Mass-transfer model. *Ind Eng Chem Res*. 1996;35(5):1660-1667.
22. Olujić Ž, Behrens M, Colli L, Paglianti A. Predicting the efficiency of corrugated sheet structured packings with large specific surface area. *Chem Biochem Eng Q*. 2004;18(2):89-96.
23. Kim I, Jens CM, Grimstvedt A, Svendsen HF. Thermodynamics of protonation of amines in aqueous solutions at elevated temperatures. *J Chem Thermodyn*. 2011;43(11):1754-1762.
24. Lide DR, ed. *CRC Handbook of Chemistry and Physics: a Ready-Reference Book of Chemical and Physical Data (84th Edition)*. CRC Press; 2003.

SUPPORTING INFORMATION

Additional supporting information can be found online in the Supporting Information section at the end of this article.

How to cite this article: Hami Dindar I, Lutters N, Kenig EY. Carbon dioxide capture by aqueous glucosamine solutions: Pilot plant measurements and a theoretical study. *AIChE J*. 2024;70(11):e18541. doi:10.1002/aic.18541